

must be changed accordingly. It was found (3) that corrosion did not begin to occur in a bridge deck until the polarized voltage had dropped to -0.55 V, which shows that the recommended -0.85 -V minimum (5) has a considerable margin of safety built into it. As a result, the minimum and maximum polarized voltages sensed by carbon probes in the coke layer are recommended as -0.80 and -1.25 V. These values still contain a safety factor.

Half-cells buried in concrete are subject to failure or erratic behavior. This was shown in test specimen 1 in which the failure rate was quite high. Similarly, in bridge decks, these cells showed variable results. The reason for this behavior is not known.

Some results have been obtained from the bridges treated with cathodic protection that suggest that half-cells located close to rebars tend to give higher readings than those located farther away from the bars. This result may appear to contradict that obtained in the laboratory test specimen in which there was no potential gradient when, with no current being applied, the polarized potential was measured by several half-cells located at different distances from the bar. This may be explained by the fact that the laboratory specimen was electrically isolated and had no connection to ground, so that the polarized voltage could not leak off. In the case of a bridge deck, this is not the case. There is always some connection through the concrete and rebars to ground, so that the voltage can leak off, slowly or rapidly, and this will give rise to a potential gradient in the deck. This effect could also be the cause of lower polarized potentials that have been measured on the undersides of bridge decks.

The use of a carbon probe in the coke and in contact with the deck tends to average the potential and removes the effect of the distance from a rebar. This averaging effect is not found when a half-cell is buried in the concrete; this cell reads only the potential at that point. Thus, the carbon probe in the coke is the preferred way to determine the polarized potential.

The amount of power required to protect a bridge deck will vary with the amount of cover over the rebars and the electrical leakage from the deck. Higher amounts of cover will require a higher applied voltage.

CONCLUSIONS

1. Carbon probes located in the coke layer and in

contact with the deck provide a good method of measuring the polarized potential on the reinforcing steel.

2. The moist coke layer acts as a half-cell and its voltage must be taken into account when measuring the polarized potential of deck rebars.

3. The recommended range of polarized potential to provide protection to the reinforcing steel is -0.80 to -1.25 V, when read by carbon probes located in the coke layer and in contact with the concrete deck.

4. Half-cells buried in the deck and used as voltage probes produce variable results and should be used cautiously.

5. Various types of half-cells can be used to control the potential-controlled rectifiers on bridges. Here the rectifier must be set, not on the theoretical value of the half-cell, but to the calibration that will provide the desired potential on the deck steel.

REFERENCES

1. R. F. Stratfull. Inhibiting the Corrosion of Steel in a Reinforced Concrete Bridge. *Corrosion*, Vol. 15, No. 6, 1959, p. 331.
2. R. F. Stratfull. Experimental Cathodic Protection of a Bridge Deck. TRB, Transportation Research Record 500, 1974, pp. 1-50.
3. H. J. Fromm and G. P. Wilson. Cathodic Protection of Bridge Decks: Study of Three Ontario Bridges. TRB, Transportation Research Record 604, 1976, pp. 38-47.
4. H. J. Fromm. Cathodic Protection of Rebar in Concrete Bridge Decks. *Materials Performance*, Vol. 16, Nov. 1977, pp. 21-28.
5. Control of External Corrosion on Underground Piping Systems. National Association of Corrosion Engineers, Standard RP-01-69.
6. D. A. Hausmann. Criteria for Cathodic Protection of Steel in Concrete Structures. *Materials Protection*, Vol. 8, No. 10, 1969, p. 23.
7. G. N. Scott. Corrosion-Protection Properties of Portland Cement. *American Water Works Association Journal*, Vol. 57, No. 8, 1965.
8. Handbook of Chemistry and Physics. Chemical Rubber Company, 48th Ed., 1968.

Publication of this paper sponsored by General Materials Section and Committee on Corrosion.

Methods of Determining Corrosion Susceptibility of Steel in Concrete

A. M. Rosenberg and J. M. Gaidis, W. R. Grace and Company, Columbia, Maryland

Several test methods were used to study the effectiveness of calcium nitrite as a corrosion inhibitor in concrete. Measurements of open-circuit potential and of polarization in concrete were found to be useful, provided the steel area studied was completely covered by concrete. Tests in which limewater was used as a substitute for concrete yielded similar results. Induced electrolysis was found to be misleading because of other reactions that occurred. Tests on large slabs [$1.8 \times 0.6 \times 0.15$ m (6×2

$\times 0.5$ ft)] that were salted daily showed that calcium nitrite reduced the corrosion susceptibility more than fourfold.

Corrosion is an electrochemical phenomenon (1). An oxide coating does not form on iron in a dry atmosphere.

Corrosion continues because the iron oxide film is not thermodynamically stable in the presence of metallic iron and moisture (2). The result is the formation of the more soluble ferrous ion, which can move away, thus exposing more iron surface to corrosion.

In concrete, where the pH of the medium is approximately 12.5, iron in the ferric state is the most stable form (3). This makes concrete one of the best rust-preventive coatings. A thin film of iron oxide acts as the cathodic part of the reinforcing bar where oxygen is reduced



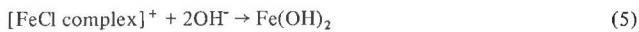
Iron goes into solution at the anode but, in concrete, it rapidly goes to the highest oxidation state as



and, by subsequent oxidation,



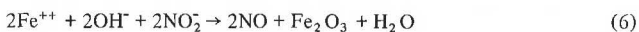
Unfortunately, this simple protection scheme offered by concrete breaks down in the presence of chloride ions. Chloride ions can penetrate the passive film on iron in concrete and carry ferrous ions away from the anodic areas as transient complexes, thus preventing polarization of the anode. In this way, considerable corrosion can take place.



and, by subsequent oxidation,



In earlier work (4), we used calcium nitrite as an admixture in concrete to prevent corrosion of iron and found that it reacts with ferrous ions as follows:



In this way, a tight protective film is produced around the iron to prevent chloride penetration and further corrosion.

To show the effects of any protective system in concrete is not simple, because the corrosion process that actually disrupts the concrete takes place over many years. Corrosion depends not only on the chloride ion concentration but also on the water content, the availability of oxygen, and the concrete itself.

Most rapid methods test only one aspect of the process. In our development of a corrosion-inhibiting admixture, we used a number of test methods previously reported in the literature.

Our testing program was divided into five different studies:

1. Measurements of the open-circuit potential of steel in concrete placed in chloride solutions,
2. Measurements of the polarization of steel in concrete placed in chloride solutions,
3. Measurements of the induced electrolysis of concrete in chloride solutions,
4. Electrical measurements of steel in limewater, and
5. Accelerated bridge-deck-corrosion tests in-

volving daily ponding with 3 percent sodium chloride solution.

TESTING PROGRAM

Open-Circuit Potential

A valuable tool for assessing whether corrosion is progressing in concrete is the measurement of the spontaneous potential of the iron versus a standard electrode (5,6). Tafel has shown that the change in measured potential (η) is proportional to the current density (i) (7)

$$\eta = \beta \log i + K \quad (7)$$

where β and K are constants. Thus, a large change in potential is approximately proportional to a large increase in current or rate of corrosion.

The open-circuit potential (E) is actually composed of several factors (see Equation 8).

$$E_{\text{open-circuit}} = E_{\text{O}_2}^0 - E_{\text{Fe}}^0 - (RT/2F) \log \{[\text{Fe}^{++}] [\text{OH}^-]^2 / P_{\text{O}_2}\} + \eta \quad (8)$$

where

R = gas constant,
 T = temperature, and
 F = Faraday's constant.

Although there are concentration changes as corrosion progresses, the major change in potential is due to η . Also, in Equation 8, the transfer coefficients of the anodic and cathodic reactions, which indicate the fraction of the additional electric field added by the activation polarization and are used to decrease the chemical activation energy of the electrode reactions, have been neglected.

The specimens were 7×7×22 cm (2.8×2.8×8.8 in) and were made from ASTM C185 mortar in 0.95-L (1-qt) waxed cardboard containers and had no. 4 rebars embedded. The specimens were cured 1 week at 24°C (75°F) and 100 percent relative humidity, and then half were immersed in saturated sodium chloride solution and the other half were dried to constant weight [4 d at 50°C (122°F) and 0 percent relative humidity] before immersion to a depth of approximately 11 cm (4.4 in). The potentials of these specimens were followed for more than 1000 h, when it became clear that all specimens, even the inhibited ones, were exhibiting active potentials. At first, this was ascribed to the accelerated nature of the test, but careful examination suggested that the rust on the protruding section of rebar might be in electrical contact with the damp concrete. Breaking several specimens apart showed that, on the whole, the uninhibited specimens and those that contained 0.5 percent $\text{Ca}(\text{NO}_2)_2$ (based on cement) had rust spots well within the concrete, but those that contained 2 percent $\text{Ca}(\text{NO}_2)_2$ as well as some of those that contained 1 percent $\text{Ca}(\text{NO}_2)_2$ were corroded only at the steel-concrete-air interface. When the specimens were sandblasted to remove a cone about 1 cm (0.4 in) deep and this was filled with epoxy, the potentials decreased up to 200 mV for those specimens that had the larger quantities of inhibitor.

Polarization

When an external negative potential is impressed on iron beyond the normal corrosion levels, an insulating film forms over the surface and the corrosion rate decreases. Thus, by impressing a potential across steel embedded in concrete, we can study the relationship

Figure 1. Polarization diagram.

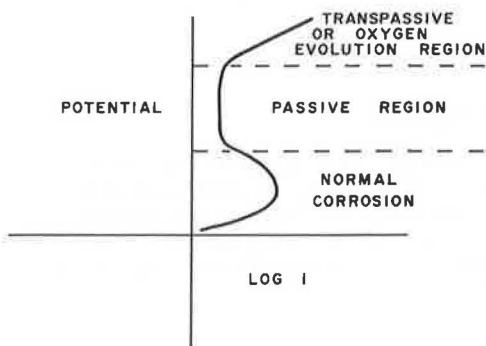
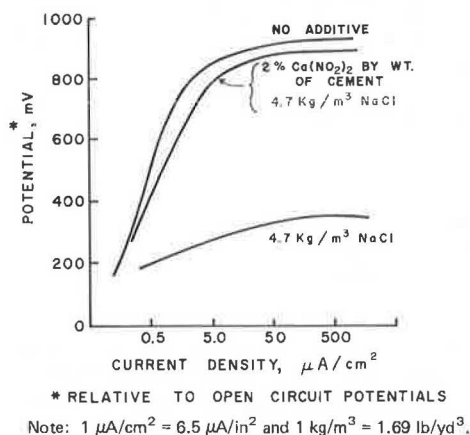


Figure 2. Polarization of steel in concrete.



Note: 1 $\mu\text{A}/\text{cm}^2 = 6.5 \mu\text{A}/\text{in}^2$ and 1 $\text{kg}/\text{m}^3 = 1.69 \text{ lb}/\text{yd}^3$.

between potential and corrosion rate (see Figure 1).

Mortar (prepared according to the recipe of ASTM C185 but using concrete sand) was cast into 10.2×20.3-cm (4×8-in) molds around no. 4 reinforcing bars that had been sandblasted. After curing for 7 d, the specimens were subjected to impressed anodic currents of 0.05 to 200 mA over the whole iron area [approximately 20 cm^2 (3 in^2)], and the change from the open-circuit potential was measured. Figure 2 shows the potential versus current density curves for specimens tested in saturated NaCl solution immediately after moist curing for 1 week and for specimens containing 4.7 kg/m^3 (8 lb/yd^3) of NaCl and tested in saturated NaCl solution after 1 week of moist curing.

Induced Electrolysis

Because corrosion is an electrochemical phenomenon that leads to the destruction of concrete over a period of many years, it seems logical to speed up the process by externally increasing the voltage to increase the rate, which would enable the whole process to be studied in several months.

Thus, specimens similar to those used for the polarization studies were cured 28 d, then soaked in 5 percent NaCl solution for 28 d, and subjected to 10 V of impressed potential in saturated NaCl solution.

Limewater as a Substitute for Concrete

Although a solution of limewater can never duplicate the environment inside concrete (which changes over the years), it does show the corrosion susceptibility of steel at a pH of 12.5. And indeed, the slope of a plot of volt-

Table 1. Concrete properties of bridge decks.

Ca(NO ₂) ₂ (percent by weight of cement)	Water-to- Cement Ratio	Slump (cm)	Air (percent)	Compressive Strength (MPa)		
				3 d	7 d	28 d
Series 1						
0		11.1	5.5	19.96	24.0	31.0
1		12.1	6.4	21.6	25.4	35.0
2		10.2	4.8	25.1	28.3	39.2
3		10.8	4.9	28.3	33.9	43.8
Series 2						
0	0.57	12.1	4.5	15.1	19.2	24.8
1	0.57	7.6	5.8	16.6	20.4	26.4
2	0.56	8.25	4.6	21.6	25.5	31.1
Series 3						
0		15.2	2.0	18.5	24.4	32.4
1	0.61	13.3	1.9	18.7	26.4	33.8
2	0.62	15.2	2.8	19.7	29.1	36.3
Series 4						
0	0.53	14.0	5.8	21.3	28.9	35.3
2	0.55	14.0	5.2	24.4	33.7	43.1
Series 5						
0	0.57	10.2	4.8			
1	0.58	9.5	5.2			
2	0.59	12.7	4.8			

Note: 1 cm = 0.4 in and 1 MPa = 145 lb/in^2 .

age versus current is the same in limewater and in concrete (8).

Thus, no. 3 reinforcing bars were totally immersed in aqueous solutions containing various amounts of NaCl and Ca(NO₂)₂ and containing excess calcium hydroxide. The bars were removed after 1 h for determination of open-circuit potential and polarization.

Accelerated Bridge-Deck-Corrosion Tests

Probably the closest way to approximate the actual corrosion process is to construct bridge decks and salt them daily. This procedure was pioneered by the Federal Highway Administration (9) and the California Department of Transportation. This is a highly exaggerated test because the salting is daily, the steel is 5.1 cm (2 in) on centers, and the concrete cover is only 2.5 cm (1 in) thick. Thus, five series of concrete decks were constructed. Each deck was 1.8×0.6×0.15 m (6×2×0.5 ft). Each series contained decks that had 0, 1, and 2 percent Ca(NO₂)₂ by weight of the cement. The series are described below:

1. Ready-mix concrete that contained an air-entraining agent,
2. Small-batch concrete that contained an air-entraining agent,
3. Small-batch concrete that did not contain an air-entraining agent,
4. Small-batch concrete that contained an air-entraining agent and a water-reducing agent [decks only at 0 and 2 percent Ca(NO₂)₂], and
5. Small-batch concrete that contained an air-entraining agent (repeat of series 2).

All slabs were formulated along the design of the Federal Highway Administration, cast, cured, fitted with dams, and then treated with 3 percent NaCl solution daily. The undersides of the decks were fitted with skirts (essentially upside-down dams) to prevent run-off NaCl solution from traveling around to the bottom of the deck and causing corrosion there. Plastic feet on the chairs used to support the rebars also helped to keep the bottoms free of corrosion and spalling. Two rebar mats were used; the upper one consisted of no. 5 rebars on 5.1-cm (2-in) centers. A connection to the rebars was taped and then potted in silicone caulking

Figure 3. Open-circuit potentials of reinforcing steel in mortar.

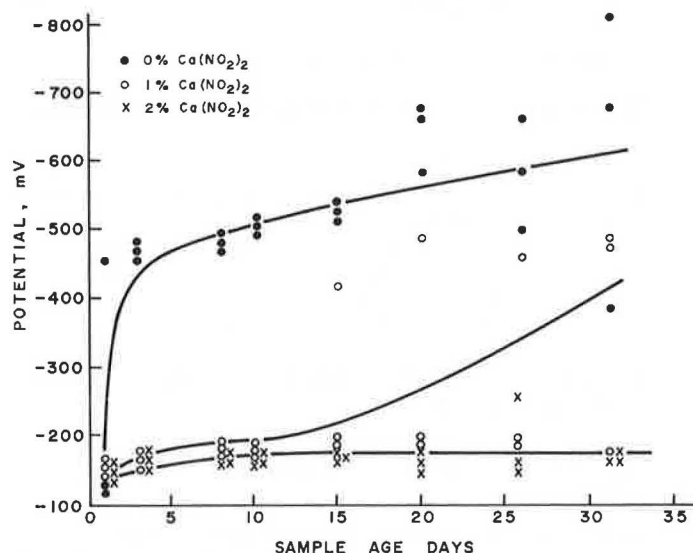
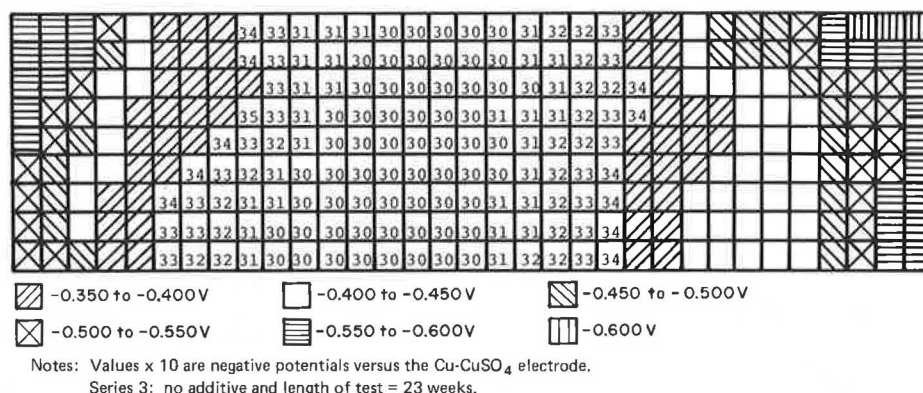


Figure 5. Voltage distribution : experimental bridge deck.



compound. The concrete properties of the decks are given in Table 1.

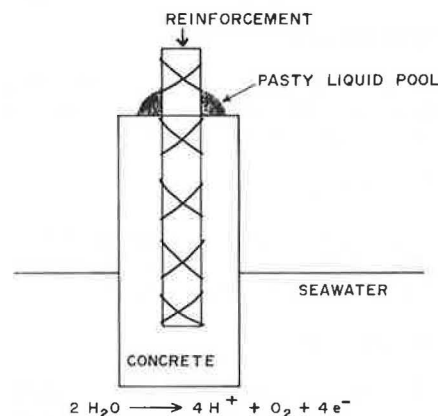
Open-Circuit Potential Measurements

Before making the open-circuit measurements on the decks, the salt solution was swept off and the decks were flushed with clean water and sponge dried. After 15 min to 1 h, depending on wind and temperature conditions, the decks had dried to the point where the concrete was still damp, but the sheen of water was gone. A commercial copper-copper sulfate reference electrode was connected through an autoranging digital voltmeter to the rebar mat by means of the wire attached before the concrete was poured. A sponge, approximately 3×3×3 cm (1.2×1.2×1.2 in), soaked in 3 percent NaCl solution was attached to the porous cap of the reference cell, and the potentials were measured on each deck. The decks were mapped by dividing them into a 9 by 33 grid of 5.1×5.1-cm squares.

X-Ray Measurements

Ten 35.6×52.6-cm (14×17-in) x-ray pictures were taken of selected concrete slabs. The irradiation source was 3.7 TBq (100 curies) of iridium-192 in a 2.5×2.5-mm (0.1×0.1-in) cylinder. The energies of the gamma rays were 0.50 and 7.5 aJ (310 and 470 keV). The x-ray

Figure 4. Induced electrolysis.



pictures show the positions of the rebars, tie wires, furniture, and voids.

Sonic Testing

Sonic testing was attempted by using ultrasonic-pulse-velocity test equipment. Although it appeared that gross abnormalities could be recognized easily, the method was premature for the degree of concrete deterioration we have encountered to date.

Chloride Analysis

After 6 months of daily salting, a 76×23-cm (30×9-in) portion of one deck (the blank of series 2) was sawed off and brought inside for further examination. Holes were drilled in 1.2- and 2.2-cm (0.5- and 0.87-in) depth increments by using a carbide bit and, after extraction, the concrete dust was analyzed by Volhard titration. Then, the top 2.5 cm of concrete was removed by hammer and chisel. Areas of corrosion were noted by discolorations in the concrete and on the steel.

Corrosometer Probes

Corrosometer probes were hung below the rebars and insulated from them at a mean depth of 5.1 cm. Readings were taken weekly.

RESULTS

Open-Circuit Potential

Figure 3 shows the open-circuit potentials we obtained after we corrected for the corrosion taking place on the steel outside the concrete.

Polarization

Figure 2 compares the polarization results we obtained when $\text{Ca}(\text{NO}_2)_2$ was used in the mortar with the results obtained when it was not used.

Induced Electrolysis

All of the samples, whether or not they contained $\text{Ca}(\text{NO}_2)_2$, ruptured after about 1 week of electrolysis at 10 V. The rupture was in most cases preceded by

a green pasty liquid that rose to the top of the concrete, as shown in Figure 4.

Limewater as a Substitute for Concrete

The results we obtained in limewater are shown below.

$\text{Ca}(\text{NO}_2)_2$ (%)	Potential (mV)			
	No NaCl	0.3 Percent NaCl	1.0 Percent NaCl	3.0 Percent NaCl
0	210	380	418	545
0.3	219	204	217	315
1.0	205	194	212	245
3.0	210	206	233	253

Here it can be seen that $\text{Ca}(\text{NO}_2)_2$ maintains the potential in the passive region.

Accelerated Bridge-Deck-Corrosion Tests

In Figure 5, the type of data that was collected from our five series of decks is shown. Previously, we had established the relationship shown in Figure 6 between the potential and the instantaneous corrosion rate.

Thus, we have chosen to show our results on these series of decks in terms of the corrosion rate, the summary of which is shown in Figure 7. These data were collected after about 6 months of daily salting, which is comparable to more than 7 years of salting on the roads in Kansas (9). The data collected 1 month later showed a very slight increase in overall corrosion. The lower temperatures in the winter will probably retard corrosion.

The data collected on a regular basis from each deck were analyzed by computer. Our goal was to use these data to predict a useful lifetime. The data were reduced from 297 data points for each deck to 33. The first analysis is shown in Figures 8 and 9.

This method of data compilation shows that the domains of the concretes that do not have an admixed corrosion inhibitor overlap, although there is some variability from series to series. However, among the domains of the decks that contain 2 percent $\text{Ca}(\text{NO}_2)_2$, there are two distinct groups and, when we compare the strength data for these decks (given in Table 1) with these results, it appears that $\text{Ca}(\text{NO}_2)_2$ is more effective with higher strength concrete. When series 2 and 5 are

Figure 6. Linear polarization.

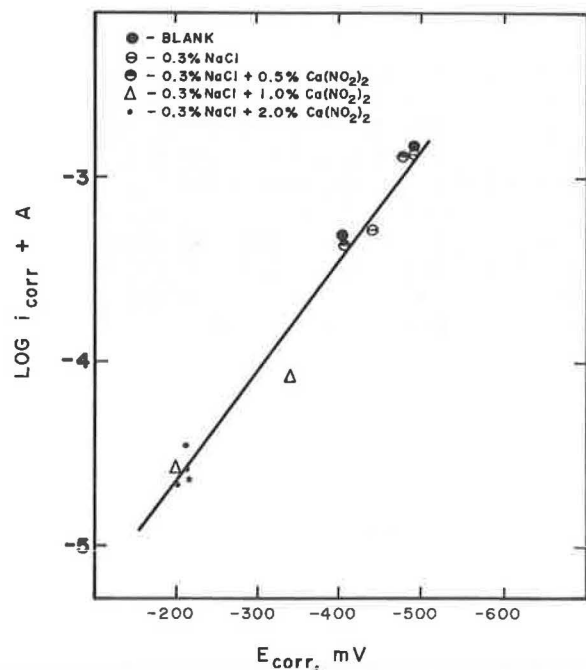


Figure 7. Average rate of corrosion as determined by potential distribution in experimental bridge decks.

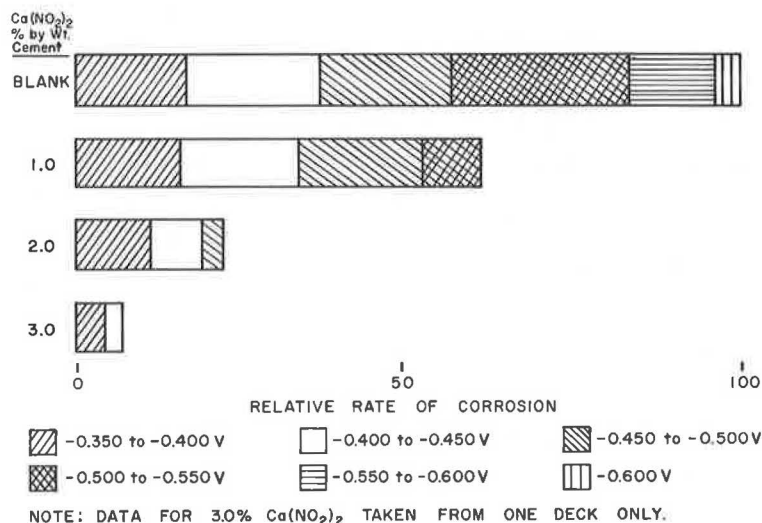


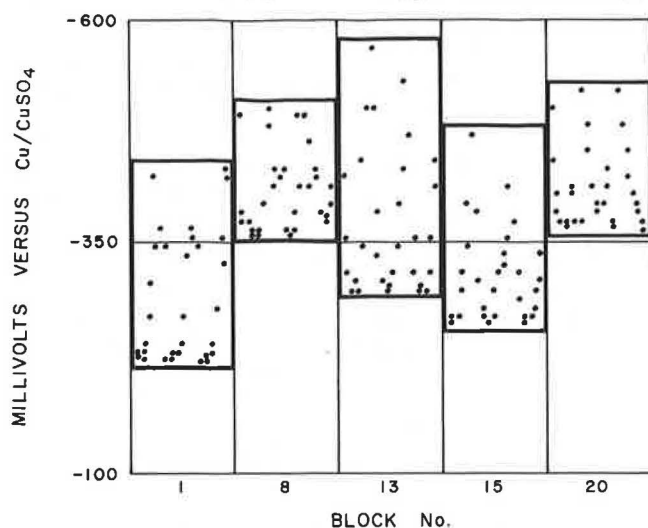
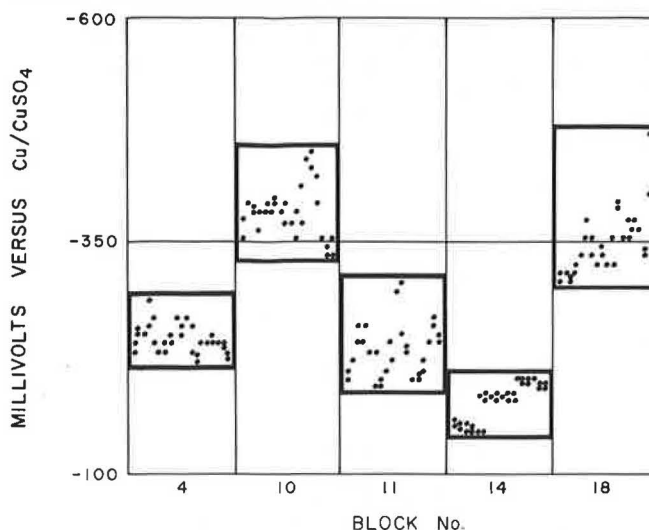
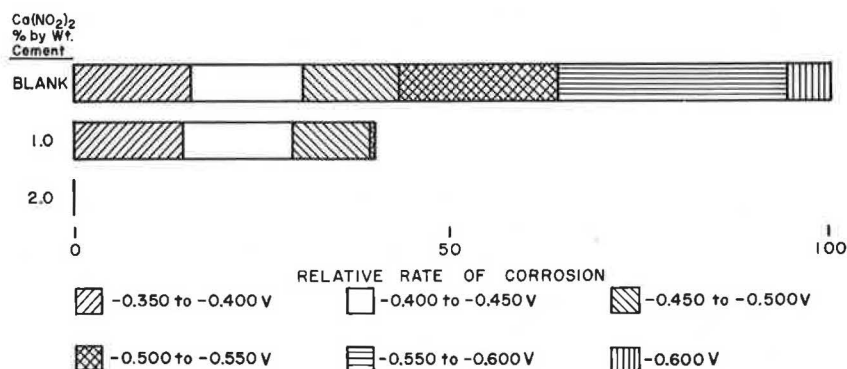
Figure 8. First data analysis : concrete containing 0 percent $\text{Ca}(\text{NO}_2)_2$.Figure 9. First data analysis : concrete containing 2 percent $\text{Ca}(\text{NO}_2)_2$.

Figure 10. Normalized rate of corrosion obtained by using data from high-strength series (1, 3, and 4) only.



eliminated, the summary of the data becomes as shown in Figure 10.

At present, we are planning to construct more decks to confirm this finding. We determined that the chloride ion concentration was 5.9 kg/m^3 (10 lb/yd^3) at the depth of the steel and that the corroded area was in the immediate vicinity of the highest potential reading obtained. This is in agreement with our previous findings (8).

The x-rays of the decks were not clear enough to be related to the corrosion. The same seems to be true of the sonic testing also. There was not enough of a difference in the small areas examined to warrant further investigation. The corrosion probes in the concrete have not shown significant changes.

DISCUSSION OF RESULTS

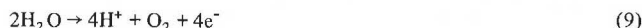
The open-circuit potential that was measured in concrete can be considered to be composed of several contributions (see Equation 8).

The standard potentials do not change. The potential contribution due to the change in concentration of ferrous and hydroxide ions is relatively small. The large change noted in this study is due to the corrosion-process contribution (see Equation 7). Although it is presumed that, once started, the corrosion process continues, there were no data found in this study to relate actual life times of concrete structures to electrical measurements of samples. Stratfull has found that there is a relationship between high potential readings and eventual cracking of the concrete (11). Andrade (12) found, in

prestressed concrete that contained 2 percent calcium chloride by mass of cement, that the nitrite inhibitor was still effective after 5.5 years of testing.

Polarization curves show that a passive film will form on iron in concrete. It appears from Figure 3 that a protective coating on steel in concrete can form only when chloride is not present or when both chloride and calcium nitrite are present.

Although corrosion is an electrochemical phenomenon, speeding up the process by induced electrolysis is not recommended because, as the potential is increased, the reactions in concrete change. Rather than the corrosion reaction shown in Equation 2, water is electrolyzed



and hydrogen ions are produced. Hartt and Turner (13) found that, when they put samples under constant current or a high potential, the pH measurements of the solutions that oozed to the top ranged from less than 0 to an upper limit of 4. Not only will the H^+ and O_2 produced damage the iron in the concrete and at the top of the sample, but also the acid will destroy the concrete itself.

Testing in limewater has proved valuable because the results correlate well with those found in concrete. In the accelerated bridge-deck-corrosion testing, there appears to be a correlation between the strength of the concrete and the effectiveness of calcium nitrite. When only concrete that has a 28-d compressive strength of more than 34.5 MPa (5000 lbf/in^2) is con-

sidered, the inhibitor-containing concrete is free of corrosion. This is not too unusual because strong concrete will aid the formation of a tight passive film on the steel. In weaker concrete, where some signs of corrosion are apparent even when $\text{Ca}(\text{NO}_2)_2$ is present, inhibited concrete still shows less corrosion than the unprotected concrete.

CONCLUSIONS

Accelerated tests for determining the corrosion susceptibility of iron in concrete, such as

1. Open-circuit-potential measurements in concrete,
2. Polarization measurements in concrete, and
3. Similar electrical measurements in limewater,

show that $\text{Ca}(\text{NO}_2)_2$ offers effective corrosion protection.

Induced electrolysis of concrete is not a reliable technique for studying a corrosion inhibitor when electrolysis of water takes place.

Large deck tests confirm the effectiveness of $\text{Ca}(\text{NO}_2)_2$ as a corrosion inhibitor in concrete after 6 months of daily salting. Because this is an accelerated-test procedure, the use of $\text{Ca}(\text{NO}_2)_2$ as an inhibitor should lead to many years of corrosion-free concrete.

REFERENCES

1. H. H. Uhlig. *Corrosion and Corrosion Control*. Wiley, New York, 1971, p. 1.
2. D. Gilroy and J. E. O. Mayne. *British Corrosion Journal*, Vol. 1, Nov. 1965, pp. 102-106.
3. W. M. Latimer. *Oxidation Potentials*. Prentice-Hall, New York, 2nd Ed., 1952, p. 228.
4. A. M. Rosenberg, J. M. Gaidis, T. G. Kossivas, and R. W. Previte. ASTM, Special Technical Publication 629, 1977, pp. 89-99.
5. K. C. Clear. *Rebar Corrosion in Concrete: Effect of Special Treatments*. ACI, Publication SP-49, 1975, pp. 71-82.
6. R. F. Stratfull, W. J. Jurkovich, and D. L. Spellman. *Corrosion Testing of Bridge Decks*. Paper presented at the 54th Annual Meeting, TRB, 1975; California Transportation Laboratory, Res. Rept. CA-DOT-TL-5116-12-75-03, 1975.
7. H. H. Uhlig. *Corrosion and Corrosion Control*. Wiley, New York, 1971, p. 45.
8. J. T. Lundquist, Jr., A. M. Rosenbert, and J. M. Gaidis. *A Corrosion Inhibitor Formulated With Calcium Nitrite for Chloride-Containing Concrete: II—Improved Electrochemical Test Procedure*. Paper presented at National Association of Corrosion Engineers Meeting, San Francisco, 1977.
9. K. C. Clear and R. E. Hay. *Time-to-Corrosion of Reinforcing Steel in Concrete Slabs*. Federal Highway Administration, Rept. RD-73-32, April 1973.
10. B. F. McCollom. *Design and Construction of Conventional Bridge Decks That Are More Resistant to Spalling*. TRB, Transportation Research Record 604, 1976, pp. 1-5.
11. R. F. Spellman. *Half-Cell Potentials and the Corrosion of Steel in Concrete*. California Department of Public Works, Division of Highways, Res. Rept. CA-HY-MR-5116-7-72-42, Nov. 1972.
12. C. Andrade. *The Inhibitive Action of Different Quantities of NaNO_2* . Cuadernos de Investigacion, Instituto Eduardo Torroja de la Construcción y del Cemento, Madrid, No. 30, 1974, p. 15.
13. D. H. Turner. *Cracking of Concrete Due to Corrosion of Various Embedded Metals*. College of Engineering, Florida Atlantic University, Boca Raton, thesis, 1976.

Publication of this paper sponsored by Committee on Corrosion.

Measurement of Cement Content by Using Nuclear Backscatter-and-Absorption Gauge

Terry M. Mitchell, Office of Research, Federal Highway Administration

The delays inherent in current methods for the quality control of portland cement concrete allow large volumes to be placed before problems are discovered. This paper discusses an instrument and a test method for obtaining early quality information: The device is a nuclear backscatter-and-absorption gauge that measures the cement content of plastic concrete. The paper includes a description of the device, a summary of two laboratory evaluation studies, and a discussion of the data obtained by using the gauge on five highway construction projects. Laboratory evaluations established the accuracy of the gauge, its field worthiness and dependence on aggregate composition, and its lack of dependence on concrete density, temperature, and other batching variables. The results showed accuracies of $\pm 13 \text{ kg/m}^3$ ($\pm 22 \text{ lb/yd}^3$) for most siliceous aggregate mixes and $\pm 18 \text{ kg/m}^3$ ($\pm 31 \text{ lb/yd}^3$) for calcareous aggregate mixes. In most cases, nuclear-gauge determinations on the field sites agreed with

calculated cement factors established from batch tickets. Discrepancies encountered on two of the field projects are discussed. The major limitations of the gauge are the necessity for recalibration whenever the aggregate source or the ratio of coarse to fine aggregates is changed and its reduced accuracy for calcareous and certain siliceous aggregates.

The need for early-age composition measurements on portland cement concrete is becoming more and more evident. Reliance on compressive-strength tests made 7 or 28 d after placement can allow large quantities of pavement or structural concrete to be placed before defects are discovered. Accelerated strength tests, which